

MindDrive: A Vision-Language-Action Model for Autonomous Driving via Online Reinforcement Learning

Haoyu Fu^{1*}, Diankun Zhang^{2*}, Zongchuang Zhao¹, Jianfeng Cui²,
Hongwei Xie^{2†}, Bing Wang², Guang Chen², Dingkan Liang^{1†}, Xiang Bai¹

¹ Huazhong University of Science and Technology, ² Xiaomi EV
{hyfu, zcuangzhao, dkliang, xbai}@hust.edu.cn
<https://xiaomi-mlab.github.io/MindDrive/>

Abstract

Current Vision-Language-Action (VLA) paradigms in autonomous driving primarily rely on Imitation Learning (IL), which introduces inherent challenges such as distribution shift and causal confusion. Online Reinforcement Learning offers a promising pathway to address these issues through trial-and-error learning. However, applying online reinforcement learning to VLA models in autonomous driving is hindered by inefficient exploration in continuous action spaces. To overcome this limitation, we propose MindDrive, a VLA framework comprising a large language model (LLM) with two distinct sets of LoRA parameters. The one LLM serves as a Decision Expert for scenario reasoning and driving decision-making, while the other acts as an Action Expert that dynamically maps linguistic decisions into feasible trajectories. By feeding trajectory-level rewards back into the reasoning space, MindDrive enables trial-and-error learning over a finite set of discrete linguistic driving decisions, instead of operating directly in a continuous action space. This approach effectively balances optimal decision-making in complex scenarios, human-like driving behavior, and efficient exploration in online reinforcement learning. Using the Qwen-0.5B LLM, MindDrive achieves a Driving Score (DS) of 78.04 and a Success Rate (SR) of 55.09% on the challenging Bench2Drive benchmark. To the best of our knowledge, this is the first work to demonstrate the effectiveness of online reinforcement learning for the VLA model in autonomous driving.

1. Introduction

Autonomous driving (AD) relies on the model’s ability to perceive, make decisions, and act in dynamic and complex

* Equal contribution. † Project leader. Work done when Haoyu Fu was working as an intern at Xiaomi EV.

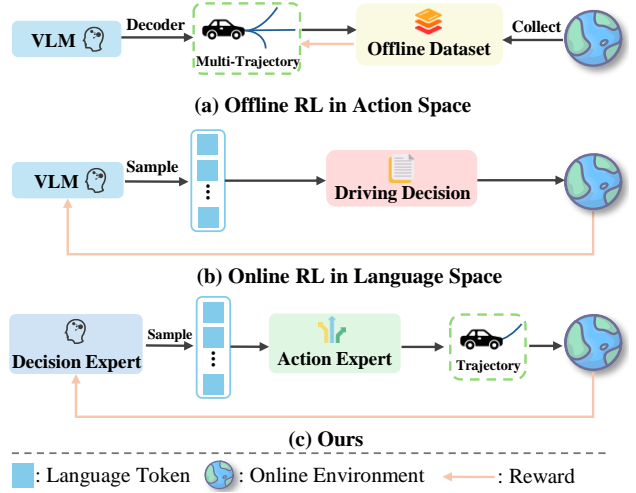


Figure 1. The comparison of different VLA for reinforcement learning (RL) paradigms. The Decision and Action Experts share a base VLM but employ distinct LoRA adapters. MindDrive uses the Action Expert to map the Decision Expert’s linguistic inferences to concrete trajectories and refines the model’s reasoning ability online by leveraging action rewards.

environments. Traditional end-to-end autonomous driving frameworks [14, 25, 58] integrate perception, prediction, and planning modules, but they lack common sense and causal reasoning abilities. With the improved visual understanding and reasoning ability of Vision Language Models (VLMs) [1, 2, 46], many research [10, 40, 52] attempts to apply the Vision-Language-Action (VLA) paradigm to the field of end-to-end AD. The VLA paradigm in autonomous driving aims to translate complex traffic scene understanding into trajectories of the ego vehicle.

Current VLA models [10, 17, 51] are predominantly trained using imitation learning (IL), which aims to fit expert behaviors from collected driving data. However, exclu-

sive reliance on the IL paradigm renders models susceptible to causal confusion and distributional shift [7, 41], resulting in irreversible error accumulation in closed-loop driving scenarios. Reinforcement learning offers a perspective for addressing these challenges through trial-and-error and has achieved notable success in enhancing the causal reasoning capabilities of VLMs [12, 36, 39].

Unlike reinforcement learning in VLMs’ discrete language space, the action space of autonomous driving is a continuous trajectory space. Applications of reinforcement learning in the current VLA domain for autonomous driving can be categorized into two main paradigms: offline reinforcement learning for the action space and online reinforcement learning for the language space. Offline reinforcement learning is typically trained on fixed datasets composed of expert demonstrations, as shown in Fig. 1 (a). These methods [24, 30, 56, 64, 64] employ offline reinforcement learning with distinct reward functions [6] to generate more feasible trajectories in the action space. Although they made great progress, offline reinforcement learning restricts the VLA model’s ability to explore by interacting with the environment. Additionally, the optimization of trajectories in reinforcement learning cannot effectively optimize the reasoning ability of VLMs. To overcome these limitations, some other methods [16, 26] attempt to employ online reinforcement learning in the language space, as shown in Fig. 1 (b). These methods treat the driving decision as the action and facilitate a deeper understanding of causal reasoning through online reinforcement learning, but they struggle to map driving decisions to specific and human-like driving trajectories effectively. Therefore, utilizing online reinforcement learning to enhance the performance of autonomous driving VLA requires further exploration.

To address these challenges, we propose a novel architecture, MindDrive, a VLA model for autonomous driving via online reinforcement learning, as shown in Fig. 1 (c). MindDrive transforms the action space from trajectories into language-based decisions by dynamically mapping, significantly improving exploration efficiency while using trajectory rewards to reinforce the model’s reasoning in online reinforcement learning. Specifically, MindDrive consists of two homogeneous LLMs that differ only in their respective LoRA adapters [13]. One LLM acts as a Decision Expert, responsible for making reasonable decisions based on the current scenario, while the other serves as an Action Expert, establishing a dynamic mapping from the reasoning result to continuous trajectories. MindDrive first leverages IL to establish a one-to-one correspondence between the meta-actions inferred by the Decision Expert and the multi-modal trajectories output by the Action Expert. The high-quality driving trajectories output by the Action Expert provide reasonable and human-style candidates for online reinforcement learning. Subsequently, we utilize on-

line reinforcement learning to refine the Decision Expert, allowing it to learn how to make the correct decision by sampling different trajectories and receiving corresponding reward signals from the online interactive environment.

Meanwhile, to enable model exploration and training in a dynamic, interactive environment, we introduce an online closed-loop reinforcement learning framework for autonomous driving VLA models, built upon the CARLA simulator [8]. We define explicit signals for task success and failure, and partition the online reinforcement learning process into data collection and training phases. During collection, we compute and cache scene tokens for each frame, which serve as compact state representations. This pre-computation step reduces memory buffer overhead, enables large-batch training, and allows the entire process to be formulated as a standard Markov Decision Process [38].

We evaluate the driving ability of MindDrive on the comprehensive and challenging closed-loop benchmark, Bench2Drive [22]. Extensive experiments demonstrate that our framework leads to more effective driving behavior in complex driving scenarios. Notably, even with a lightweight 0.5B LLM model, MindDrive achieves a Driving Score (DS) of 78.04 and a Success Rate (SR) of 55.09%, outperforming the strong baseline model [10] in the same size parameter by 5.15 and 9.26%, respectively.

The main contributions of this paper are as follows:

- We propose MindDrive, an online reinforcement learning framework for VLA autonomous driving models. By introducing a dynamic language-action mapping, MindDrive significantly improves exploration efficiency and enables trajectory-level action rewards to facilitate reasoning optimization.
- We introduce a computationally efficient online reinforcement learning scheme. To the best of our knowledge, MindDrive is the first VLA-based autonomous driving model to be trained with online reinforcement learning in a simulator, aiming to bring new inspiration to the autonomous driving community.
- Extensive experiments demonstrate the effectiveness of MindDrive, achieving 78.04 DS and 55.09% SR on the Bench2Drive benchmark, substantially outperforming the state-of-the-art IL baseline at the same model scale.

2. Related work

2.1. End-to-End Autonomous Driving (AD)

End-to-end (E2E) autonomous driving (AD) based on imitation learning [14, 21, 25, 37] integrates perception, prediction, and planning into a differentiable framework [5, 34, 35, 57]. These models directly map sensor inputs to trajectories or control commands from expert data. Representative methods such as UniAD [14] and VAD [25] adopt dense bird’s-eye view (BEV) representations to unify mul-

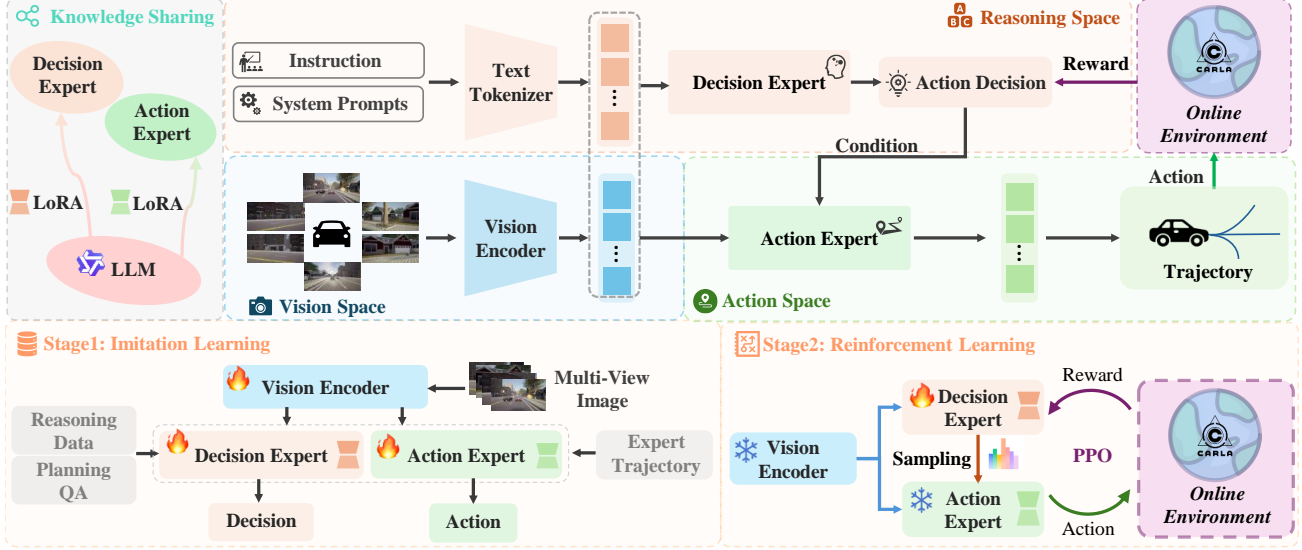


Figure 2. Overview of MindDrive and its training pipeline. MindDrive consists of two experts, both of which utilize the same base LLM and fine-tune with distinct LoRA parameters, respectively. Decision Expert generates high-level meta-actions from scene and text inputs, and Action Expert maps these meta-actions to concrete trajectories. MindDrive is first trained with Imitation Learning (IL) on expert data to align meta-actions with trajectories. Then it is refined through online reinforcement learning in a closed-loop simulator, where action rewards directly enhance the model’s reasoning capabilities.

tiple tasks. Generative approaches, including GenAD [61] and DiffusionDrive [32], employ diffusion-based planning for multi-modal trajectory generation. DiffAD [48] rasterizes heterogeneous driving targets into a unified BEV space for joint optimization, while MomAD [45] introduces momentum modeling for stability. SparseAD [58] and DriveTransformer [23] improve efficiency with sparse queries.

Despite strong open-loop results, E2E models often fail in closed-loop due to distribution shift and causal confusion [4, 22]. To overcome these limitations, recent studies have explored the integration of vision-language models (VLMs) for AD, leveraging their strong generalization, reasoning abilities, and world knowledge. HERMES [62] proposes a unified model of the AD world, integrating 3D scene understanding and future generation for the first time. DriveGPT4 [51], ELM [63], DriveMonkey [60] and DriveMM [15] incorporate VLMs for perception, prediction, and decision-making. OmniDrive [47], EMMA [17], and OpenEMMA [50] represent trajectories as text with chain-of-thought reasoning [49]. AutoVLA [64] discretizes actions for alignment with language models but struggles with continuous motion.

VLA models from embodied AI, such as OpenVLA [27] and the π series [3, 18], extend to continuous action spaces. ORION [10] connects language and action via a generative planner for continuous trajectories, improving reasoning and generalization in the autonomous driving scenarios. However, imitation learning is still limited in effectively propagating trajectory-level supervision into the high-level reasoning space of language models. MindDrive advances

this line by integrating online reinforcement learning for adaptive interaction and robust decision-making.

2.2. Reinforcement Learning for AD

Reinforcement learning (RL) has achieved notable success ranging from LLMs [12] to complex games [31], and is increasingly applied in AD. CarPlanner [59] applies expert-guided rewards for stable learning, while RAD [11] and R2SE [33] enhance closed-loop training and avoid forgetting. Raw2Drive [55] employs a dual-stream model-based RL to align raw and privileged world models. Recent works such as AlphaDrive [26], AutoVLA [64], and RecogDrive [30] adopt GRPO-based RL [12] to refine planning through reward engineering. However, most rely on offline expert datasets and handcrafted rewards, lacking actual interaction with the environment. Online RL enables adaptive decision-making via trial-and-error learning but faces slow convergence and inefficient exploration. Our approach addresses these issues through adaptive online RL, which improves closed-loop robustness and decision quality.

3. Method

In this section, we present our proposed MindDrive in detail. As illustrated in Fig. 2, MindDrive architecture consists of two main components: a Decision Expert and an Action Expert, which share a common Vision Encoder and Text Tokenizer but differ only in their respective LoRA parameters [13]. The Decision Expert performs high-level reasoning from navigation instructions and multi-view vi-

sual inputs, generating abstract driving decisions in the form of meta-actions. The Action Expert translates these meta-actions into concrete action trajectories, conditioned on the scene information and instruction. This design enables flexible and interpretable action generation, bridging high-level reasoning with low-level control.

Our training process includes two stages: 1) Imitation learning (IL) establishes a mapping between language and action space (Sec. 3.2), providing high-quality candidate trajectories for online Reinforcement learning (RL) and effectively reducing its exploration space. 2) Online RL further enhances the model’s comprehension ability through action rewards in an online environment (Sec. 3.3).

3.1. Problem Formulation

In the task of end-to-end autonomous driving, we aim to generate a diverse trajectory set A and determine an optimal trajectory a^* based on surrounding visual information V and language instructions L :

$$\begin{aligned} A &= \{a_i\}_{i=1}^N, \text{ where } a_i \sim \pi_g(a \mid V, L), \\ a^* &= \arg \max_{a \in A} \pi_g(a \mid V, L), \end{aligned} \quad (1)$$

where a_i represents the trajectory in the multimodal trajectory set A and $\pi_g(a \mid V, L)$ is the trajectory generation policy function. Current methods often select the optimal trajectory based on the score-based selection policy π_c :

$$a^* = \arg \max_{a \in A} \pi_c(a). \quad (2)$$

To fully leverage the potential of the VLA model, we model the selection task as an action decision process and introduce $\pi_d(a \mid V, L)$ as the selection policy function:

$$\begin{aligned} a^* &= \arg \max_{a \in A} \pi_c(a) \\ &= \arg \max_{a \in A} \underbrace{\pi_d(a \mid V, L)}_{\text{selection}} \cdot \underbrace{\pi_g(a \mid V, L)}_{\text{generation}}. \end{aligned} \quad (3)$$

From Eq. 3, we can clearly identify that the generation of the optimal trajectory depends on two core policy functions: π_d and π_g . Previous methods fail to establish a connection between these two policy spaces in online reinforcement learning. To address this challenge, we establish a mapping relationship from linguistic meta-actions to trajectories, and then leverage the trajectory feedback to optimize the reasoning of π_d through online reinforcement learning. **Online RL** enables the model to continuously learn and optimize its policy through dynamic interaction with the environment, which is crucial for enhancing the model’s understanding of causal relationships. We model our trajectory decision process tasks as a Markov Decision Process (MDP) [55, 59] for online reinforcement learning. The MDP is

structured as a tuple $\langle S, A, P, R, \gamma \rangle$. The state $s_t \in S$ represents all necessary information for the agent to decide at step t . The model selects an action from the action space A according to the policy (π_d, π_g) . Following an action, the system transitions to a new state s_{t+1} according to dynamics implicitly defined by closed-loop simulation environment. The reward $r_t \in R(s_t)$ is a scalar feedback signal that evaluates the quality of executing action in state s_t . Our objective is to learn a decision-making policy π_d that maximizes the expected cumulative discounted reward in the collected data τ , guided by the discount factor γ . This objective is formulated as:

$$J(\theta) = \mathbb{E}_{\tau \sim \pi_d} [R(\tau)] = \mathbb{E}_{\tau \sim \pi_d} \left[\sum_{t=0}^{T-1} \gamma^t r_t \right]. \quad (4)$$

3.2. Language-Action Mapping

To enhance the synergy between our decision-making π_d and trajectory generation policy π_g , we decouple a single LLM into two specialized experts with different LoRA parameters. One LLM serves as the Decision Expert, implementing the policy π_d , while the other acts as the Action Expert, responsible for the policy π_g . This architecture ensures they operate from a shared foundation of world knowledge while performing their distinct functions. We first leverage IL to create a mapping between the Decision Expert and the Action Expert to establish a connection between language and action and enhance the exploration efficiency in the subsequent reinforcement process.

Inspired by [40, 52], we decouple the control into longitudinal and lateral control to improve planning flexibility and design the corresponding meta-action in planning QA. We generate the planning QA pairs using LLMs and refine them through manual filtering to ensure a one-to-one correspondence between language and actions (see the Appendix for details). The model is then trained on both the reasoning data and planning QA to learn the mapping from language to action. The loss function can be expressed as:

$$\mathcal{L}_{CE} = -\frac{1}{N} \sum_{i=1}^N \sum_{t=1}^{T_i} \log P(y_{i,t} | x_i, y_{i,<t}). \quad (5)$$

Then, we map the meta-actions to the temporal speed trajectory for longitudinal control and the geometric path trajectory for lateral control in Action Expert. Specifically, we leverage the autoregressive nature of the Action Expert to encode visual and language information into a hidden state \mathbf{x} and introduce two special tokens, `<speed.waypoints>` and `<path.waypoints>`, to extract the logits from the Action Expert’s output:

$$P_\theta(\mathbf{x}) = \prod_{k=1}^K P_\theta(\mathbf{x}_k \mid \mathbf{x}_{<k}). \quad (6)$$

Finally, we utilize a Variational Autoencoder (VAE) [28] with a GRU-based decoder to align our language and action spaces, directly translating visual-language representations into the final action trajectory:

$$p(z|x) \sim N(\mu_x, \sigma_x^2), \pi_g(a|V, L) = gru(z), \quad (7)$$

where z is gaussian variables in the latent space.

We utilize the common detection loss \mathcal{L}_{det} for auxiliary supervision [10]. The VAE is trained by a Kullback-Leibler divergence loss under the supervision of expert trajectories. We employ L1 loss as the behavior cloning loss for speed and path waypoint regression. The total loss is:

$$\mathcal{L}_{\pi}^{il}(\theta) = \mathcal{L}_{BC} + \mathcal{L}_{CE} + \mathcal{L}_{vae} + \mathcal{L}_{det}. \quad (8)$$

3.3. Online RL for Action-Reasoning

IL generates human-like trajectories but often suffers from causal confusion. To overcome this, we leverage online RL within the CARLA simulator [8]. As shown in Fig. 3, this online approach enables the agent to explore the environment through trial and error, learning from direct interaction and consequences, thereby bolstering the model’s driving performance in complex scenarios. To leverage prior knowledge from IL, the value network shares the same weights as the LLM, with the only difference being that its final layer is replaced by a Multi-Layer Perceptron (MLP) to predict the state value.

To achieve an efficient rollout process, we deployed N parallel CARLA collectors, focusing on routes with different scenarios that the model failed to complete after IL. At each step, we use a vision encoder to process the visual information in the scene and convert it into state embeddings. We query the Decision Expert in the form of a question and sample from its output logits about meta-action tokens. The sampling meta-actions further map to precise trajectories in the action space by the Action Expert. Meanwhile, the value network is used to estimate the value of the current state at each decision step.

Given that MindDrive has already acquired basic driving skills through IL pre-training, we employ a sparse reward function to guide the optimization of its high-level reasoning space. Specifically, a reward of +1 is assigned when the vehicle successfully reaches its destination, while a reward of -1 is incurred when a predefined penalty event is triggered. For all other normal driving scenarios, the reward is 0. The reward function r_t is defined as follows:

$$r_t = \begin{cases} +1 & \text{if the destination is reached} \\ -1 & \text{if a penalty event is triggered} \\ 0 & \text{otherwise} \end{cases} \quad (9)$$

We use the official CARLA [8] leaderboard metrics as our penalty event. The penalty events include major infractions, such as collisions with other vehicles and running a

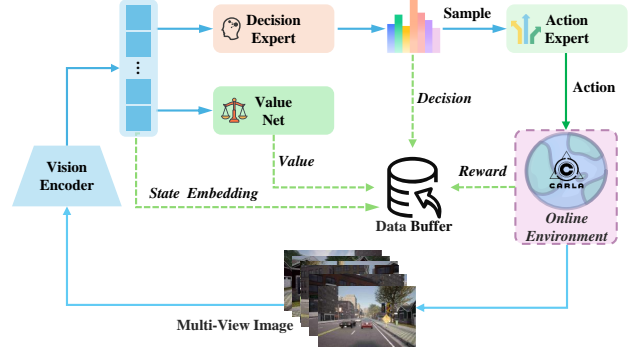


Figure 3. Online reinforcement learning framework. The RL pipeline records per-scenario state embeddings, value estimates, decisions, and action rewards into the data buffer.

red light (see more details in Exp. 4.3). The rollout process will be terminated once any penalty event is triggered.

After collecting a complete route, the δ value is calculated by the Temporal-Difference method:

$$\delta_t = r_t + \gamma \cdot V'(s_{t+1}) - V'(s_t), \quad (10)$$

where V' is the value network function, and γ is the discount factor to ensure future rewards are appropriately weighted in the decision-making process. Then we calculate GAE (Generalized Advantage Estimation):

$$\hat{G}_t = \delta_t + \gamma \lambda \cdot \hat{G}_{t+1}, \quad (11)$$

where λ is the trace-decay parameter that controls the bias-variance trade-off in advantage estimation.

Instead of directly using multi-images for RL training, we use the state embedding extracted by the vision encoder to represent the current state. This approach can simultaneously integrate temporal and visual information and improve computational efficiency by avoiding repeated computation. We store the value, decision-action, and reward of each step into a data buffer.

Upon collecting all routes into the rollout buffer, we optimize the policy π_d using the Proximal Policy Optimization (PPO) algorithm [42]:

$$\mathcal{L}_{ppo} = \mathbb{E}_t \left[\min \left(\frac{\pi_d}{\pi_{d,old}} G_t, \text{clip} \left(\frac{\pi_d}{\pi_{d,old}}, 1 - \epsilon, 1 + \epsilon \right) G_t \right) \right], \quad (12)$$

where ϵ is the clipping parameter in PPO. Benefit from the proposal RL training framework, MindDrive is able to be trained in a large batch for stable optimization.

Meanwhile, to mitigate the problem of catastrophic forgetting during the reinforcement learning fine-tuning phase, we introduce a Kullback-Leibler divergence loss as a regularization term. This loss function is designed to constrain the output distribution of the meta-actions of the Decision Expert. Its formula can be expressed as:

$$\mathcal{L}_{KL} = D_{KL}(P_{ref}(\cdot|s) \parallel P_{\theta}(\cdot|s)). \quad (13)$$

During training, only the parameters of the MLP head within the value net are updated. The optimization is performed by minimizing the Mean Squared Error (MSE) loss, formulated as:

$$\mathcal{L}_{V'}(\theta) = \frac{1}{N} \sum_{t=1}^N (V_{\theta}(s_t) - G_t)^2. \quad (14)$$

Finally, the online reinforcement policy learning loss is:

$$\mathcal{L}_{\pi}^{\text{rl}}(\theta) = \mathcal{L}_{ppo} + \mathcal{L}_{V'} + \beta \mathcal{L}_{KL}, \quad (15)$$

where β is a coefficient that controls the strength of the KL regularization.

4. Experiments

4.1. Experimental Settings

Dataset. We train and evaluate MindDrive on the Bench2Drive dataset [22], a comprehensive closed-loop benchmark for autonomous driving (AD) based on the CARLA simulator [8]. During imitation learning (IL), we adopt the official base set of 1000 clips, with 950 used for training and 50 for open-loop validation. We perform closed-loop evaluation on the official Bench2Drive benchmark, including 220 short routes across 44 interactive scenarios. For the online reinforcement learning (RL), we selected 44 routes that the model successfully completed through action sampling (see the Appendix for details).

Metrics. For closed-loop evaluation, we adopt three key metrics: Driving Score (DS), Success Rate (SR), and Multi-Ability. Following the CARLA benchmark [8], the SR measures the proportion of routes completed within the specified time limit, and the DS is based on route completion but is reduced by penalties for infractions. Multi-Ability independently evaluates five advanced urban driving skills.

Model Setting. In imitation learning, we set the number of speed waypoints $\mathbf{w}_s \in \mathbb{R}^{N_s \times 2}$ to $N_s = 6$, representing a future 3-second trajectory sampled at 2Hz. For the path waypoints $\mathbf{w}_p \in \mathbb{R}^{N_p \times 2}$ $N_p = 20$ points are used to define a 20-meter path with a 1-meter interval between consecutive points. We use QT-former as our vision encoder [10]. The decision space for the Decision VLM includes 7 speed meta-actions and 6 path meta-actions, aligning with the downstream planning trajectory. The detailed definitions of the meta-actions are provided in the Appendix.

Training Process. All experiments are conducted on 32 NVIDIA A800 GPUs with 80 GB of memory. We employ EVA-02-L [9] as the vision encoder. We use the lightweight Qwen2-0.5B [53] as our base LLM. We apply Chat-B2D [10] as our reasoning data and perform joint training with planning QA pairs. Both experts are fine-tuned with LoRA [13], the rank dimension and alpha set to 16. In the RL stage, data is collected in parallel using 24

Carla simulations. We train for 10 epochs on the collected data. For more training details, see the Appendix.

4.2. Main Results

We conduct a comprehensive comparison between MindDrive and representative methods from both the traditional end-to-end (E2E) and vision-language-action (VLA) paradigms on the Bench2Drive benchmark. Tab. 1 lists the detailed results, and we find that:

1) MindDrive delivers promising performance with a lightweight model. Compared with the traditional E2E methods, MindDrive surpasses the latest SOTA IL model DiffAD [48] by 10.12 DS and 16.45% SR, and the offline RL-based method Raw2Drive [55] by 6.68 DS and 4.85% SR. Within the VLA paradigm, MindDrive achieves comparable performance to the SOTA IL-based ORION [10] and outperforms DriveMoE [54] by 3.82 DS and 6.45% SR. Notably, using the lightweight Qwen2-0.5B, MindDrive achieves competitive performance, in contrast to the substantially larger LLMs employed by ORION and DriveMoE (*i.e.*, Vicuna1.5-7B and Paligemma-3B), highlighting our method’s superior efficiency.

2) Online RL enhances MindDrive’s capability in complex dynamic interactions. As shown in Tab. 1, MindDrive demonstrates a clear advantage over other methods. It surpasses the offline RL-based RecogDrive [30] by 6.68 DS and 9.64%SR, and MindDrive-IL by 2.19 DS and 5.79% SR, strongly validating the superiority of the proposed online RL paradigm. The Multi Ability metric further supports this finding. Specifically, MindDrive achieves a 14.91% improvement in mean ability over RecogDrive [30] and 5.57% over the IL method ORION with the same lightweight LLM. Notably, it achieves substantial gains in capabilities closely tied to meta-actions selection, with improvements of 55.56% in Overtaking and 30% in Give Way. Although MindDrive performs lower than the SOTA VLA methods in the Emergency Brake and Traffic Sign ability, it still exhibits a noticeable advantage over our MindDrive-IL, with improvements of 8.33% and 0.98%, respectively. These results confirm that online RL significantly strengthens the model’s causal reasoning and decision-making robustness in complex interactive environments.

4.3. Ablation Studies

In ablation studies, two online RL rollouts are performed per route unless specified otherwise.

Ablation on Penalty Events. We introduce four penalty events during the online RL stage: collisions with pedestrians or vehicles, running a red light, driving off-road or deviating over 30 meters from the route, and failing to obey a stop sign (*i.e.*, Collision, Traffic Light, Route Deviation, and Stop, respectively). We assign a sparse reward of -1 to penalize our model for triggering these events. As shown

Table 1. Closed-loop and Multi-Ability Results of E2E-AD Methods in Bench2Drive under **base** training set. C/L refers to camera/LiDAR. * denote expert feature distillation. † represent reproducing the result based on official code. DS: Driving Score, SR: Success Rate, M: Merging, O: Overtaking, EB: Emergency Brake, GW: Give Way, TS: Traffic Sign.

| Method | LLM | Reference | Modality | Scheme | Closed-loop | | Ability (%) ↑ | | | | | |
|---------------------------------|--------------|------------|----------|------------|--------------|--------------|---------------|--------------|--------------|--------------|--------------|--------------|
| | | | | | DS↑ | SR(%)↑ | M | O | EB | GW | TS | Mean |
| Traditional End-to-End Paradigm | | | | | | | | | | | | |
| TCP-traj* | - | NeurIPS 22 | C | IL | 59.90 | 30.00 | 8.89 | 24.29 | 51.67 | 40.00 | 46.28 | 34.22 |
| ThinkTwice* [20] | - | CVPR 23 | C | IL | 62.44 | 31.23 | 27.38 | 18.42 | 35.82 | 50.00 | 54.23 | 37.17 |
| DriveAdapter* [19] | - | ICCV 23 | C&L | IL | 64.22 | 33.08 | 28.82 | 26.38 | 48.76 | 50.00 | 56.43 | 42.08 |
| UniAD-Base [14] | - | CVPR 23 | C | IL | 45.81 | 16.36 | 14.10 | 17.78 | 21.67 | 10.00 | 14.21 | 15.55 |
| VAD [25] | - | ICCV 23 | C | IL | 42.35 | 15.00 | 8.11 | 24.44 | 18.64 | 20.00 | 19.15 | 18.07 |
| GenAD [61] | - | ECCV 24 | C | IL | 44.81 | 15.90 | - | - | - | - | - | - |
| MomAD[45] | - | CVPR 25 | C | IL | 44.54 | 16.71 | - | - | - | - | - | - |
| WoTE [29] | - | ICCV 25 | C&L | IL | 61.71 | 31.36 | - | - | - | - | - | - |
| DriveTransformer-Large [23] | - | ICLR 25 | C | IL | 63.46 | 35.01 | 17.57 | 35.00 | 48.36 | 40.00 | 52.10 | 38.60 |
| DiffAD [48] | - | arXiv 25 | C | IL | 67.92 | 38.64 | 30.00 | 35.55 | 46.66 | 40.00 | 46.32 | 38.79 |
| DriveDPO [43] | - | NeurIPS 25 | C | Offline RL | 62.02 | 30.62 | - | - | - | - | - | - |
| Raw2Drive [55] | - | NeurIPS 25 | C | Offline RL | 71.36 | 50.24 | 43.35 | 51.11 | 60.00 | 50.00 | 62.26 | 53.34 |
| Vision-Language-Action Paradigm | | | | | | | | | | | | |
| Driveπ0 [54] | Paligemma-3B | arXiv 25 | C | IL | 60.45 | 30.00 | 29.35 | 36.58 | 48.83 | 40.00 | 54.45 | 41.84 |
| DriveMoE [54] | Paligemma-3B | arXiv 25 | C | IL | 74.22 | 48.64 | 34.67 | 40.00 | 65.45 | 40.00 | 59.44 | 47.91 |
| ORION [10] | Vicuna-7B | ICCV 25 | C | IL | 77.74 | 54.62 | 25.00 | 71.11 | 78.33 | 30.00 | 69.15 | 54.72 |
| ORION [10] | Qwen2-0.5B † | ICCV 25 | C | IL | 72.89 | 45.83 | 26.32 | 62.22 | 55.55 | 50.00 | 63.30 | 51.37 |
| RecogDrive [30] | Qwen2.5-7B | arXiv 25 | C | Offline RL | 71.36 | 45.45 | 29.73 | 20.00 | 69.09 | 20.00 | 71.34 | 42.03 |
| MindDrive-IL | Qwen2-0.5B | - | C | IL | 75.85 | 49.30 | 30.26 | 66.67 | 60.00 | 33.33 | 56.91 | 49.44 |
| MindDrive | Qwen2-0.5B | - | C | Online RL | 78.04 | 55.09 | 32.89 | 75.56 | 68.33 | 50.00 | 57.89 | 56.94 |

Table 2. Ablation on different penalty events. C: Collision, TL: Traffic Light, RD: Route Deviation, S: Stop. M: Merging, O: Overtaking, EB: Emergency Brake, GW: Give Way, TS: Traffic Sign, DS/SR: Driving Score/Success Rate.

| ID | Penalty Events | | | | Closed-loop \uparrow | | Ability (%) \uparrow | | | | | |
|----|----------------|----|----|---|------------------------|--------------|------------------------|-------|-------|-------|-------|--------------|
| | C | TL | RD | S | DS | SR(%) | M | O | EB | GW | TS | Mean |
| 1 | | | | | 75.85 | 49.30 | 30.26 | 66.67 | 60.00 | 33.33 | 56.91 | 49.44 |
| 2 | ✓ | | | | 75.41 | 50.70 | 28.00 | 71.11 | 60.00 | 50.00 | 56.91 | 53.20 |
| 3 | ✓ | ✓ | | | 76.02 | 51.47 | 31.42 | 57.77 | 68.97 | 50.00 | 58.43 | 53.32 |
| 4 | ✓ | ✓ | ✓ | | 76.95 | 51.85 | 27.63 | 73.33 | 65.00 | 50.00 | 57.36 | 54.67 |
| 5 | ✓ | ✓ | ✓ | ✓ | 78.04 | 55.09 | 32.89 | 75.56 | 68.33 | 50.00 | 57.89 | 56.94 |

in Tab. 2, the progressive incorporation of these penalties leads to consistent improvements in both the success rate and mean driving ability score over the IL baseline (ID-1).

Specifically, introducing the collision penalty (ID-2) yields a 1.4% SR and 3.76% mean ability improvement over the IL baseline (ID-1), while maintaining a comparable DS. In overtaking scenarios, MindDrive demonstrates exceptional performance, outperforming the baseline (ID-1) by a significant margin of 4.44%. We attribute this improvement to the model’s learned ability to adopt a more proactive strategy for collision avoidance in the continuous and interactive traffic flow. However, this strategic shift consequently impairs its merging performance.

Incorporating the traffic-light penalty (ID-3) brings further improvements over the IL baseline (ID-1), elevating

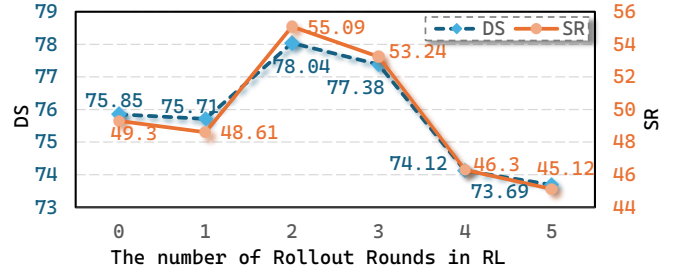


Figure 4. Ablation on the rollout rounds number. DS and SR denote Driving Score and Success Rate, respectively.

Traffic Sign by 1.52% and Emergency Braking by 8.97%. However, conflicting reward signals within this penalty lead to a noticeable drop in overtaking performance. Introducing a route-deviation penalty (ID-4) helps achieve a better trade-off between decisiveness and caution, although the stricter constraints on exploration limit further performance gains. Notably, adding a stop sign penalty significantly boosts overall performance, as it strongly correlates with the stop meta-action, enabling more effective policy learning. This is especially beneficial in merging scenarios that feature stop signs, yielding improvements of 5.26% in Merging ability and 3.24% in the SR compared to ID-4.

Without complex reward engineering, MindDrive could discover effective driving policies through online trial and error, autonomously learning from failures to progressively determine the optimal actions.

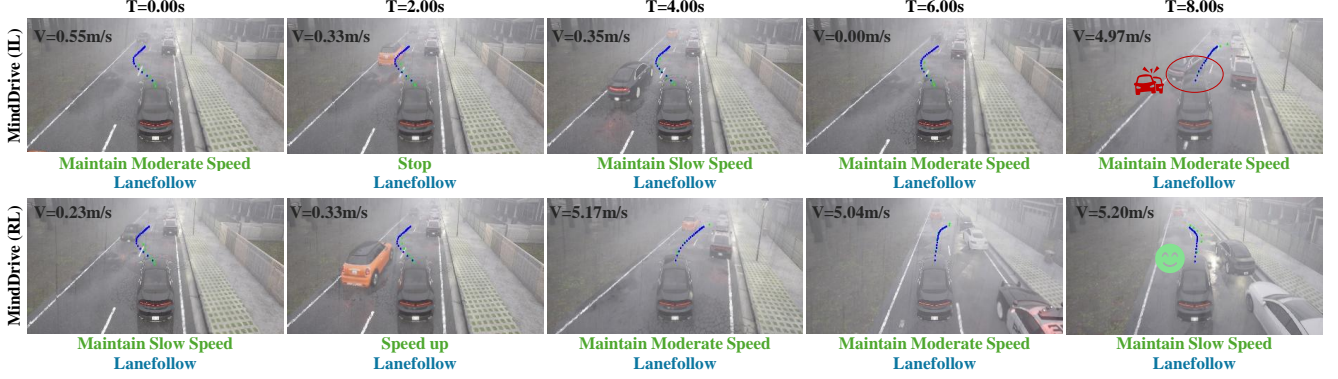


Figure 5. Qualitative results of MindDrive after IL and RL on the Bench2Drive closed-loop evaluation set. The green and blue refer to the prediction speed and path meta-actions, respectively. Red denote a collision has occurred.

Table 3. Effectiveness of different policy regularization methods. DS and SR denote Driving Score and Success Rate separately.

| Policy Regularization | DS \uparrow | SR(%) \uparrow |
|-----------------------|---------------|------------------|
| PPO-Vanilla | 74.73 | 46.73 |
| PPO-Entropy | 75.71 | 49.24 |
| PPO-KL | 78.04 | 55.09 |

Ablation on the Number of Rollout Rounds. We further analyze the sensitivity of MindDrive to the number of rollout rounds during online RL. As shown in Fig. 4, when only a single rollout is performed, the value network’s inaccurate estimation leads to erroneous advantage estimates for each action, resulting in a performance drop compared to the baseline. After executing two rollouts, our model significantly outperforms the baseline, improving DS by 2.19 and SR by 5.79%. However, further increasing rollouts substantially degrades performance, with DS dropping from 78.04 to 73.69 and SR declining from 55.09% to 45.12%. We attribute this degradation to catastrophic forgetting, where excessive rollouts cause the policy to overfit recent experiences and forget previously learned scene understanding. Therefore, we set the default rollout round number to 2, balancing exploration efficiency and training stability.

Ablation on Policy Regularization. We evaluate different policy regularization methods within PPO, as shown in Tab. 3. Our method outperforms vanilla PPO by 3.31 DS and 8.36% SR, demonstrating that KL divergence loss effectively stabilizes policy updates during RL training and mitigates catastrophic forgetting. Compared to entropy-based regularization (PPO-Entropy), our approach improves by 2.33 DS and 5.85% SR, indicating that while entropy regularization promotes exploration, excessive policy stochasticity is suboptimal for goal-directed driving tasks. Overall, our KL regularization method leads to more efficient learning, characterized by a faster policy optimization process and higher sample efficiency than baselines.

Ablation on Control Method. We finally investigate

Table 4. Ablation on the control method. DS and SR denote Driving Score and Success Rate separately.

| Control Method | DS \uparrow | SR(%) \uparrow |
|-------------------------|---------------|------------------|
| Navigation Command (IL) | 68.11 | 41.59 |
| Meta Action (IL) | 75.85 | 49.30 |
| Meta Action (RL) | 78.04 | 55.09 |

the effect of different control methods by comparing two high-level instruction approaches: navigation commands and LLM-generated meta actions. As detailed in Tab. 4, the VLM-guided meta-actions IL model achieves 7.74 DS and 7.71% SR improvements over the navigation-command baseline, indicating that VLM-derived meta-actions enable more effective reasoning in complex traffic scenarios. Employing online RL further improves meta-actions selection, yielding additional gains of 2.19 DS and 5.79% SR.

4.4. Qualitative Results

We present a qualitative comparison between the IL and RL versions of MindDrive in Fig. 5. The IL paradigm exhibits strong task-specific competence, such as issuing timely stop commands for early braking. However, IL-only MindDrive struggles in dynamic and interactive scenarios, especially in those requiring complex decision-making (e.g., determining the optimal timing for lane changes). After RL training, MindDrive selects more robust meta-actions in challenging scenarios, resulting in safer and more decisive lane-change behaviors. These qualitative results demonstrate that the RL stage substantially enhances the VLM’s high-level reasoning and decision-making capabilities, enabling it to handle complex and uncertain traffic environments better.

5. Conclusion

In this paper, we introduce **MindDrive**, a novel autonomous driving framework that leverages language as an interface for online reinforcement learning (RL). MindDrive maps language instructions to actions, transforming exploration

space into a discrete language space to reduce RL costs. It also enables the Large Language Model to refine its reasoning through action feedback in a closed-loop simulator. We conduct experiments within our proposed online RL training framework. Experiments show MindDrive achieves state-of-the-art performance with a lightweight model. To our knowledge, this is the first work to successfully train a Vision-Language-Action model for autonomous driving in an interactive simulator. We expect this work will provide valuable insights for the autonomous driving community.

Limitations. Due to the absence of real world interactive simulators, our evaluation is restricted to the CARLA simulator [8]. Additionally, the challenge of synchronizing multiple CARLA simulators precludes the evaluation of alternative actions from an identical initial state, restricting our application of the GRPO algorithm [44].

References

- [1] Josh Achiam, Steven Adler, Sandhini Agarwal, Lama Ahmad, Ilge Akkaya, Florencia Leoni Aleman, Diogo Almeida, Janko Altschmidt, Sam Altman, Shyamal Anadkat, et al. Gpt-4 technical report. *arXiv preprint arXiv:2303.08774*, 2023. 1
- [2] Rohan Anil, Sebastian Borgeaud, Yonghui Wu, Jean-Baptiste Alayrac, Jiahui Yu, Radu Soricut, Johan Schalkwyk, Andrew M Dai, Anja Hauth, Katie Millican, et al. Gemini: A family of highly capable multimodal models. *arXiv preprint arXiv:2312.11805*, 1, 2023. 1
- [3] Kevin Black, Noah Brown, Danny Driess, Adnan Esmail, Michael Equi, Chelsea Finn, Niccolo Fusai, Lachy Groom, Karol Hausman, Brian Ichter, et al. π_0 : A vision-language-action flow model for general robot control. *arXiv preprint arXiv:2410.24164*, 2024. 3
- [4] Holger Caesar, Varun Bankiti, Alex H Lang, Sourabh Vora, Venice Erin Liong, Qiang Xu, Anush Krishnan, Yu Pan, Giancarlo Baldan, and Oscar Beijbom. nuscenes: A multimodal dataset for autonomous driving. In *Proc. of IEEE Intl. Conf. on Computer Vision and Pattern Recognition*, pages 11621–11631, 2020. 3
- [5] Jie Cheng, Yingbing Chen, Xiaodong Mei, Bowen Yang, Bo Li, and Ming Liu. Rethinking imitation-based planners for autonomous driving. In *Proc. of the IEEE Int. Conf. on Robotics and Automation*, pages 14123–14130, 2024. 2
- [6] Daniel Dauner, Marcel Hallgarten, Tianyu Li, Xinshuo Weng, Zhiyu Huang, Zetong Yang, Hongyang Li, Igor Gilitschenski, Boris Ivanovic, Marco Pavone, et al. Navsim: Data-driven non-reactive autonomous vehicle simulation and benchmarking. In *Proc. of Advances in Neural Information Processing Systems*, pages 28706–28719, 2024. 2
- [7] Pim De Haan, Dinesh Jayaraman, and Sergey Levine. Causal confusion in imitation learning. *Proc. of Advances in Neural Information Processing Systems*, 32, 2019. 2
- [8] Alexey Dosovitskiy, German Ros, Felipe Codevilla, Antonio Lopez, and Vladlen Koltun. Carla: An open urban driving simulator. In *Proc. of IEEE Intl. Conf. on Robot Learning*, pages 1–16, 2017. 2, 5, 6, 9
- [9] Yuxin Fang, Quan Sun, Xinggang Wang, Tiejun Huang, Xinlong Wang, and Yue Cao. Eva-02: A visual representation for neon genesis. *Image and Vision Computing*, 149:105171, 2024. 6
- [10] Haoyu Fu, Diankun Zhang, Zongchuang Zhao, Jianfeng Cui, Dingkan Liang, Chong Zhang, Dingyuan Zhang, Hongwei Xie, Bing Wang, and Xiang Bai. Orion: A holistic end-to-end autonomous driving framework by vision-language instructed action generation. In *Proc. of IEEE Intl. Conf. on Computer Vision*, 2025. 1, 2, 3, 5, 6, 7
- [11] Hao Gao, Shaoyu Chen, Bo Jiang, Bencheng Liao, Yiang Shi, Xiaoyang Guo, Yuechuan Pu, Haoran Yin, Xiangyu Li, Xinbang Zhang, et al. Rad: Training an end-to-end driving policy via large-scale 3dgs-based reinforcement learning. In *Proc. of Advances in Neural Information Processing Systems*, 2025. 3
- [12] Daya Guo, Dejian Yang, Haowei Zhang, Junxiao Song, Ruoyu Zhang, Runxin Xu, Qihao Zhu, Shirong Ma, Peiyi Wang, Xiao Bi, et al. Deepseek-r1: Incentivizing reasoning capability in llms via reinforcement learning. *arXiv preprint arXiv:2501.12948*, 2025. 2, 3
- [13] Edward J Hu, Phillip Wallis, Zeyuan Allen-Zhu, Yuanzhi Li, Shean Wang, Lu Wang, Weizhu Chen, et al. Lora: Low-rank adaptation of large language models. In *Proc. of Intl. Conf. on Learning Representations*, 2021. 2, 3, 6
- [14] Yihan Hu, Jiazhi Yang, Li Chen, Keyu Li, Chonghao Sima, Xizhou Zhu, Siqi Chai, Senyao Du, Tianwei Lin, Wenhai Wang, et al. Planning-oriented autonomous driving. In *Proc. of IEEE Intl. Conf. on Computer Vision and Pattern Recognition*, pages 17853–17862, 2023. 1, 2, 7
- [15] Zhijian Huang, Chengjian Feng, Feng Yan, Baihui Xiao, Zequn Jie, Yujie Zhong, Xiaodan Liang, and Lin Ma. Robotron-drive: All-in-one large multimodal model for autonomous driving. In *Proc. of IEEE Intl. Conf. on Computer Vision*, pages 8011–8021, 2025. 3
- [16] Zilin Huang, Zihao Sheng, Yansong Qu, Junwei You, and Sikai Chen. Vlm-rl: A unified vision language models and reinforcement learning framework for safe autonomous driving. *Transportation Research Part C: Emerging Technologies*, 180:105321, 2025. 2
- [17] Jyh-Jing Hwang, Runsheng Xu, Hubert Lin, Wei-Chih Hung, Jingwei Ji, Kristy Choi, Di Huang, Tong He, Paul Covington, Benjamin Sapp, et al. Emma: End-to-end multimodal model for autonomous driving. *arXiv preprint arXiv:2410.23262*, 2024. 1, 3
- [18] Physical Intelligence, Kevin Black, Noah Brown, James Darpinian, Karan Dhabalia, Danny Driess, Adnan Esmail, Michael Equi, Chelsea Finn, Niccolo Fusai, et al. $\pi_{0.5}$: a vision-language-action model with open-world generalization. *arXiv preprint arXiv:2504.16054*, 2025. 3
- [19] Xiaosong Jia, Yulu Gao, Li Chen, Junchi Yan, Patrick Langechuan Liu, and Hongyang Li. Driveadapter: Breaking the coupling barrier of perception and planning in end-to-end autonomous driving. In *Proc. of IEEE Intl. Conf. on Computer Vision*, 2023. 7
- [20] Xiaosong Jia, Penghao Wu, Li Chen, Jiangwei Xie, Conghui He, Junchi Yan, and Hongyang Li. Think twice before driving: Towards scalable decoders for end-to-end autonomous

- driving. In *Proc. of IEEE Intl. Conf. on Computer Vision and Pattern Recognition*, 2023. 7
- [21] Xiaosong Jia, Shaoshuai Shi, Zijun Chen, Li Jiang, Wenlong Liao, Tao He, and Junchi Yan. Amp: Autoregressive motion prediction revisited with next token prediction for autonomous driving. *arXiv preprint arXiv:2403.13331*, 2024. 2
- [22] Xiaosong Jia, Zhenjie Yang, Qifeng Li, Zhiyuan Zhang, and Junchi Yan. Bench2drive: Towards multi-ability benchmarking of closed-loop end-to-end autonomous driving. In *Proc. of Advances in Neural Information Processing Systems*, 2024. 2, 3, 6, 1
- [23] Xiaosong Jia, Junqi You, Zhiyuan Zhang, and Junchi Yan. Drivetransformer: Unified transformer for scalable end-to-end autonomous driving. In *Proc. of Intl. Conf. on Learning Representations*, 2025. 3, 7
- [24] Anqing Jiang, Yu Gao, Yiru Wang, Zhigang Sun, Shuo Wang, Yuwen Heng, Hao Sun, Shichen Tang, Lijuan Zhu, Jinhao Chai, et al. Irl-vla: Training an vision-language-action policy via reward world model. *arXiv preprint arXiv:2508.06571*, 2025. 2
- [25] Bo Jiang, Shaoyu Chen, Qing Xu, Bencheng Liao, Jiajie Chen, Helong Zhou, Qian Zhang, Wenyu Liu, Chang Huang, and Xinggang Wang. Vad: Vectorized scene representation for efficient autonomous driving. In *Proc. of IEEE Intl. Conf. on Computer Vision*, pages 8340–8350, 2023. 1, 2, 7
- [26] Bo Jiang, Shaoyu Chen, Qian Zhang, Wenyu Liu, and Xinggang Wang. Alphadrive: Unleashing the power of vlms in autonomous driving via reinforcement learning and reasoning. *arXiv preprint arXiv:2503.07608*, 2025. 2, 3
- [27] Moo Jin Kim, Karl Pertsch, Siddharth Karamcheti, Ted Xiao, Ashwin Balakrishna, Suraj Nair, Rafael Rafailov, Ethan Foster, Grace Lam, Pannag Sanketi, et al. Openvla: An open-source vision-language-action model. *arXiv preprint arXiv:2406.09246*, 2024. 3
- [28] Diederik P Kingma. Auto-encoding variational bayes. *arXiv preprint arXiv:1312.6114*, 2013. 5
- [29] Yingyan Li, Yuqi Wang, Yang Liu, Jiawei He, Lue Fan, and Zhaoxiang Zhang. End-to-end driving with online trajectory evaluation via bev world model. In *Proc. of IEEE Intl. Conf. on Computer Vision*, 2025. 7
- [30] Yongkang Li, Kaixin Xiong, Xiangyu Guo, Fang Li, Sixu Yan, Gangwei Xu, Lijun Zhou, Long Chen, Haiyang Sun, Bing Wang, et al. Recogdrive: A reinforced cognitive framework for end-to-end autonomous driving. *arXiv preprint arXiv:2506.08052*, 2025. 2, 3, 6, 7
- [31] Zhengyang Li, Qijin Ji, Xinghong Ling, and Quan Liu. A comprehensive review of multi-agent reinforcement learning in video games. *IEEE Transactions on Games*, 2025. 3
- [32] Bencheng Liao, Shaoyu Chen, Haoran Yin, Bo Jiang, Cheng Wang, Sixu Yan, Xinbang Zhang, Xiangyu Li, Ying Zhang, Qian Zhang, et al. Diffusiondrive: Truncated diffusion model for end-to-end autonomous driving. In *Proc. of IEEE Intl. Conf. on Computer Vision and Pattern Recognition*, pages 12037–12047, 2025. 3
- [33] Haochen Liu, Tianyu Li, Haohan Yang, Li Chen, Caojun Wang, Ke Guo, Haochen Tian, Hongchen Li, Hongyang Li, and Chen Lv. Reinforced refinement with self-aware expansion for end-to-end autonomous driving. *arXiv preprint arXiv:2506.09800*, 2025. 3
- [34] Mengmeng Liu, Hao Cheng, Lin Chen, Hellward Broszio, Jiangtao Li, Runjiang Zhao, Monika Sester, and Michael Ying Yang. Laformer: Trajectory prediction for autonomous driving with lane-aware scene constraints. In *Proc. of IEEE Intl. Conf. on Computer Vision and Pattern Recognition*, pages 2039–2049, 2024. 2
- [35] Weixin Mao, Tiancai Wang, Diankun Zhang, Junjie Yan, and Osamu Yoshie. Pillarnet: Embracing backbone scaling and pretraining for pillar-based 3d object detection. *IEEE Transactions on Intelligent Vehicles*, 2024. 2
- [36] Long Ouyang, Jeffrey Wu, Xu Jiang, Diogo Almeida, Carroll Wainwright, Pamela Mishkin, Chong Zhang, Sandhini Agarwal, Katarina Slama, Alex Ray, et al. Training language models to follow instructions with human feedback. *Proc. of Advances in Neural Information Processing Systems*, 35: 27730–27744, 2022. 2
- [37] Yunpeng Pan, Ching-An Cheng, Kamil Saigol, Keuntaek Lee, Xinyan Yan, Evangelos Theodorou, and Byron Boots. Agile autonomous driving using end-to-end deep imitation learning. *Robotics: Science and Systems*, 2018. 2
- [38] Martin L Puterman. Markov decision processes. *Handbooks in operations research and management science*, 2:331–434, 1990. 2
- [39] Rafael Rafailov, Archit Sharma, Eric Mitchell, Christopher D Manning, Stefano Ermon, and Chelsea Finn. Direct preference optimization: Your language model is secretly a reward model. *Proc. of Advances in Neural Information Processing Systems*, 36:53728–53741, 2023. 2
- [40] Katrin Renz, Long Chen, Elahe Arani, and Oleg Sinavski. Simlingo: Vision-only closed-loop autonomous driving with language-action alignment. In *Proc. of IEEE Intl. Conf. on Computer Vision and Pattern Recognition*, pages 11993–12003, 2025. 1, 4
- [41] Stéphane Ross, Geoffrey Gordon, and Drew Bagnell. A reduction of imitation learning and structured prediction to no-regret online learning. In *Proc. of Intl. Conf. artificial intelligence and statistics*, pages 627–635, 2011. 2
- [42] John Schulman, Filip Wolski, Prafulla Dhariwal, Alec Radford, and Oleg Klimov. Proximal policy optimization algorithms. *arXiv preprint arXiv:1707.06347*, 2017. 5, 2
- [43] Shuyao Shang, Yuntao Chen, Yuqi Wang, Yingyan Li, and Zhaoxiang Zhang. Drivedpo: Policy learning via safety dpo for end-to-end autonomous driving. In *Proc. of Advances in Neural Information Processing Systems*, 2025. 7
- [44] Zhihong Shao, Peiyi Wang, Qihao Zhu, Runxin Xu, Junxiao Song, Xiao Bi, Haowei Zhang, Mingchuan Zhang, YK Li, Yang Wu, et al. Deepseekmath: Pushing the limits of mathematical reasoning in open language models. *arXiv preprint arXiv:2402.03300*, 2024. 9
- [45] Ziyang Song, Caiyan Jia, Lin Liu, Hongyu Pan, Yongchang Zhang, Junming Wang, Xingyu Zhang, Shaoqing Xu, Lei Yang, and Yadan Luo. Don’t shake the wheel: Momentum-aware planning in end-to-end autonomous driving. In *Proc. of IEEE Intl. Conf. on Computer Vision and Pattern Recognition*, 2025. 3, 7

- [46] Peng Wang, Shuai Bai, Sinan Tan, Shijie Wang, Zhihao Fan, Jinze Bai, Keqin Chen, Xuejing Liu, Jialin Wang, Wenbin Ge, et al. Qwen2-vl: Enhancing vision-language model's perception of the world at any resolution. *arXiv preprint arXiv:2409.12191*, 2024. 1
- [47] Shihao Wang, Zhiding Yu, Xiaohui Jiang, Shiyi Lan, Min Shi, Nadine Chang, Jan Kautz, Ying Li, and Jose M Alvarez. Omnidrive: A holistic vision-language dataset for autonomous driving with counterfactual reasoning. In *Proc. of IEEE Intl. Conf. on Computer Vision and Pattern Recognition*, pages 22442–22452, 2025. 3
- [48] Tao Wang, Cong Zhang, Xingguang Qu, Kun Li, Weiwei Liu, and Chang Huang. Diffad: A unified diffusion modeling approach for autonomous driving. *arXiv preprint arXiv:2503.12170*, 2025. 3, 6, 7
- [49] Jason Wei, Xuezhi Wang, Dale Schuurmans, Maarten Bosma, Fei Xia, Ed Chi, Quoc V Le, Denny Zhou, et al. Chain-of-thought prompting elicits reasoning in large language models. *Proc. of Advances in Neural Information Processing Systems*, 35:24824–24837, 2022. 3
- [50] Shuo Xing, Chengyuan Qian, Yuping Wang, Hongyuan Hua, Kexin Tian, Yang Zhou, and Zhengzhong Tu. Openemma: Open-source multimodal model for end-to-end autonomous driving. In *Proc. of IEEE Winter Conf. on Applications of Computer Vision*, pages 1001–1009, 2025. 3
- [51] Zhenhua Xu, Yujia Zhang, Enze Xie, Zhen Zhao, Yong Guo, Kwan-Yee K Wong, Zhenguo Li, and Hengshuang Zhao. Drivegpt4: Interpretable end-to-end autonomous driving via large language model. *IEEE Robotics and Automation Letters*, 2024. 1, 3
- [52] Zhenhua Xu, Yan Bai, Yujia Zhang, Zhuoling Li, Fei Xia, Kwan-Yee K Wong, Jianqiang Wang, and Hengshuang Zhao. Drivegpt4-v2: Harnessing large language model capabilities for enhanced closed-loop autonomous driving. In *Proc. of IEEE Intl. Conf. on Computer Vision and Pattern Recognition*, pages 17261–17270, 2025. 1, 4
- [53] An Yang, Baosong Yang, Binyuan Hui, Bo Zheng, Bowen Yu, Chang Zhou, Chengpeng Li, Chengyuan Li, Dayiheng Liu, et al. Qwen2 technical report. *arXiv preprint arXiv:2407.10671*, 2024. 6
- [54] Zhenjie Yang, Yilin Chai, Xiaosong Jia, Qifeng Li, Yuqian Shao, Xuekai Zhu, Haisheng Su, and Junchi Yan. Drivemoe: Mixture-of-experts for vision-language-action model in end-to-end autonomous driving. *arXiv preprint arXiv:2505.16278*, 2025. 6, 7
- [55] Zhenjie Yang, Xiaosong Jia, Qifeng Li, Xue Yang, Maoqing Yao, and Junchi Yan. Raw2drive: Reinforcement learning with aligned world models for end-to-end autonomous driving (in carla v2). In *Proc. of Advances in Neural Information Processing Systems*, 2025. 3, 4, 6, 7
- [56] Zhenlong Yuan, Jing Tang, Jinguo Luo, Rui Chen, Chengxuan Qian, Lei Sun, Xiangxiang Chu, Yujun Cai, Dapeng Zhang, and Shuo Li. Autodrive-r²: Incentivizing reasoning and self-reflection capacity for vla model in autonomous driving. *arXiv preprint arXiv:2509.01944*, 2025. 2
- [57] Diankun Zhang, Zhijie Zheng, Haoyu Niu, Xueqing Wang, and Xiaojun Liu. Fully sparse transformer 3-d detector for lidar point cloud. *IEEE Transactions on Geoscience and Remote Sensing*, 61:1–12, 2023. 2
- [58] Diankun Zhang, Guoan Wang, Runwen Zhu, Jianbo Zhao, Xiwu Chen, Siyu Zhang, Jiahao Gong, Qibin Zhou, Wenyan Zhang, Ningzi Wang, et al. Sparsead: Sparse query-centric paradigm for efficient end-to-end autonomous driving. *arXiv preprint arXiv:2404.06892*, 2024. 1, 3
- [59] Dongkun Zhang, Jiaming Liang, Ke Guo, Sha Lu, Qi Wang, Rong Xiong, Zhenwei Miao, and Yue Wang. Carplanner: Consistent auto-regressive trajectory planning for large-scale reinforcement learning in autonomous driving. In *Proc. of IEEE Intl. Conf. on Computer Vision and Pattern Recognition*, pages 17239–17248, 2025. 3, 4
- [60] Zongchuang Zhao, Haoyu Fu, Dingkan Liang, Xin Zhou, Dingyuan Zhang, Hongwei Xie, Bing Wang, and Xiang Bai. Extending large vision-language model for diverse interactive tasks in autonomous driving. *arXiv preprint arXiv:2505.08725*, 2025. 3
- [61] Wenzhao Zheng, Ruiqi Song, Xianda Guo, Chenming Zhang, and Long Chen. Genad: Generative end-to-end autonomous driving. In *Proc. of European Conference on Computer Vision*, pages 87–104, 2024. 3, 7
- [62] Xin Zhou, Dingkan Liang, Sifan Tu, Xiwu Chen, Yikang Ding, Dingyuan Zhang, Feiyang Tan, Hengshuang Zhao, and Xiang Bai. Hermes: A unified self-driving world model for simultaneous 3d scene understanding and generation. In *Proc. of IEEE Intl. Conf. on Computer Vision*, 2025. 3
- [63] Yunsong Zhou, Linyan Huang, Qingwen Bu, Jia Zeng, Tianyu Li, Hang Qiu, Hongzi Zhu, Minyi Guo, Yu Qiao, and Hongyang Li. Embodied understanding of driving scenarios. In *Proc. of European Conference on Computer Vision*, pages 129–148, 2024. 3
- [64] Zewei Zhou, Tianhui Cai, Seth Z Zhao, Yun Zhang, Zhiyu Huang, Bolei Zhou, and Jiaqi Ma. Autovla: A vision-language-action model for end-to-end autonomous driving with adaptive reasoning and reinforcement fine-tuning. In *Proc. of Advances in Neural Information Processing Systems*, 2025. 2, 3

MindDrive: A Vision-Language-Action Model for Autonomous Driving via Online Reinforcement Learning

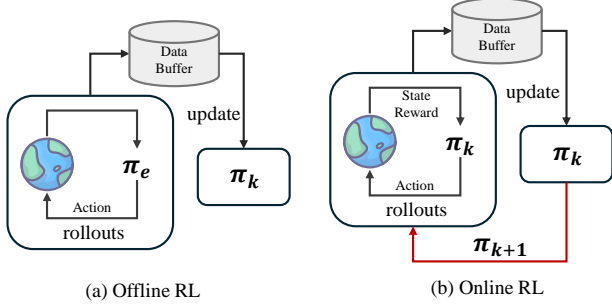


Figure A1. A Comparison of Online and Offline Reinforcement Learning (RL). π_e and π_k represent distinct policies.

We provide supplementary material to complement the main paper, arranged as follows:

- Appendix A: A Comparative Analysis of Online and Offline Reinforcement Learning.
- Appendix B: Detailed information for production planning QA.
- Appendix C: Training Details.
- Appendix D: More results.

A. Comparison of Online and Offline RL for Autonomous Driving

We compare online reinforcement learning (RL) approach with offline RL in autonomous driving, as illustrated in Fig. A1. Offline RL uses a fixed dataset collected by an expert policy π_e . The updated policy model π_k cannot be deployed into the online environment to gather new data through interaction. This paradigm often leads to causal confusion and distributional shift. In contrast, online RL deploys the updated policy π_{k+1} back into the online environment for interaction. Through trial and error in the dynamic environment, it collects new data to further strengthen the policy.

B. The Production Process of Planning QA

To construct the planning QA, we decompose the ego vehicle’s control actions into seven speed control meta-actions and six path control meta-actions. This decomposition enables more precise and flexible control in complex traffic scenarios:

- **Speed Action:** Speed Up; Slow Down; Slowdown Rapidly; Maintain Slow Speed; Maintain Moderate Speed; Maintain Fast Speed; Stop.
- **Path Action:** Turn Left; Turn Right; Change Lane Left; Change Lane Right; Straight; Lanefollow.

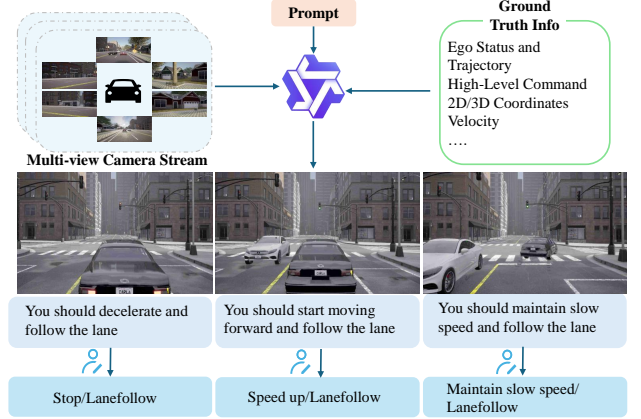


Figure A2. The production process of meta-actions. Based on consecutive frames, prompt, and the current frame’s ground truth, the VLM generates a scene action judgment, which is subsequently manually translated into meta-actions.

| | | | |
|--------------------|---------------------|---------------------|---------------------|
| RouteScenario_1773 | RouteScenario_3178 | RouteScenario_23930 | RouteScenario_25300 |
| RouteScenario_1792 | RouteScenario_3307 | RouteScenario_24041 | RouteScenario_25439 |
| RouteScenario_1956 | RouteScenario_3380 | RouteScenario_24071 | RouteScenario_25854 |
| RouteScenario_2164 | RouteScenario_3410 | RouteScenario_24098 | RouteScenario_25863 |
| RouteScenario_2201 | RouteScenario_3514 | RouteScenario_3731 | RouteScenario_26950 |
| RouteScenario_2373 | RouteScenario_14194 | RouteScenario_3785 | RouteScenario_27018 |
| RouteScenario_2397 | RouteScenario_17563 | RouteScenario_3876 | RouteScenario_27529 |
| RouteScenario_2534 | RouteScenario_17569 | RouteScenario_3904 | RouteScenario_28035 |
| RouteScenario_2554 | RouteScenario_17635 | RouteScenario_3936 | RouteScenario_28048 |
| RouteScenario_2606 | RouteScenario_23670 | RouteScenario_4468 | RouteScenario_28099 |
| RouteScenario_2989 | RouteScenario_23901 | RouteScenario_4683 | RouteScenario_28210 |

Figure A3. The collected driving scenarios for reinforcement learning rollout.

To obtain the meta-actions for each frame, we implement a two-stage data annotation pipeline, as illustrated in Fig. A2. First, we employ Qwen2VL-72B [46] to generate decision-making conditioned on the current scenario, prompt, and ground-truth information. Second, the initial action semantics output by the VLM are manually reviewed and filtered to ensure accurate alignment with standardized meta-actions, balancing comprehensiveness and precision.

We perform a statistical analysis on the generated meta-actions, as shown in Fig. A4. We collect a total of 234,769 planning QA samples. The data distribution truly reflects the statistical patterns of driving behavior in the Bench2Drive dataset [22] and comprehensively covers various actions required for safe driving.

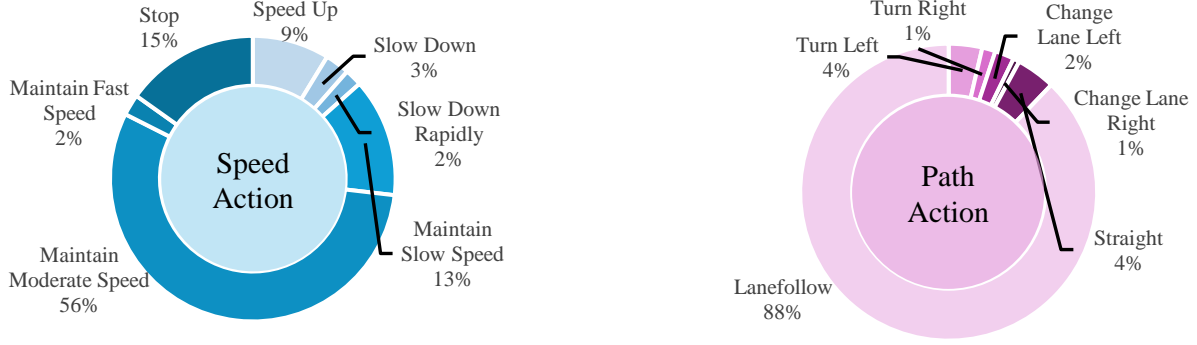


Figure A4. The statistical characteristics of meta-actions

Table A1. Hyperparameters of model architecture, PPO-related parameters, and loss weights.

| Parameter | Value |
|--------------------------|-------|
| discount factor γ | 0.99 |
| GAE parameter λ | 1.0 |
| Clip range ϵ | 0.2 |
| Batch size B | 32 |
| Weight of value loss | 0.5 |
| Weight of KL loss | 0.5 |
| Weight of PPO loss | 1 |

C. Training Details

We select 44 routes that the model is able to successfully complete through sampled actions, and each routes rollout five times. The selected routes are shown in Fig. A3.

To efficiently collect diverse and representative trajectory data, we implement a parallelized data collection framework using 24 instances of the CARLA simulator. Each simulator instance executes independent driving episodes with varied initial conditions. The episodes are terminated either upon successful task completion or when a predefined penalty condition is triggered. The data collection process takes approximately 24 hours.

Subsequently, we train the policy using the Proximal Policy Optimization (PPO) [42] algorithm. We conduct 10 epochs of training, utilizing large batches and applying advantage regularization to update the policy and value networks. The key hyperparameters, including batch size, discount factor, Generalized Advantage Estimation (GAE) lambda, and clip range, are detailed in Tab. A1.

D. More results

D.1. Analysis with a Single Expert

To highlight the effectiveness of our architecture, we conduct an ablation experiment in which a single expert is responsible for generating both the trajectory and the reasoning result during the reinforcement learning process. As

Table A2. Comparative analysis of performance on rollout routes and remain routes. DS and SR denote Driving Score and Success Rate, respectively.

| Model | Closed-loop | |
|-----------------------|---------------|------------------|
| | DS \uparrow | SR(%) \uparrow |
| <i>Rollout Routes</i> | | |
| MindDrive (IL) | 75.40 | 29.55 |
| MindDrive (RL) | 80.69 | 38.64 |
| <i>Other Routes</i> | | |
| MindDrive (IL) | 76.26 | 54.71 |
| MindDrive (RL) | 77.33 | 59.41 |

shown in Fig. A5, we observe that using a single expert adversely affects the trajectory output under our sparse reward setting, leading to catastrophic forgetting and reduction in the quality of the generated trajectory. This observation also strongly validates the advantage of our framework, which decouples reasoning from action and leverages action-based rewards to guide the optimization of reasoning.

D.2. Experiments on Rollout Routes

To evaluate the effectiveness of reinforcement learning, we analyze the model’s driving performance over both the rollout routes and the remaining routes. As shown in Tab. A2, after reinforcement learning, the model not only achieves higher success rates on the rollout routes set but also shows improvements on the other paths. Specifically, along the rollout routes, our model outperforms imitation learning by 5.29 in driving score and 9.09% in driving success rate, demonstrating its ability to make superior driving decisions by trial-and-error experience. On the remaining routes, our model still achieves improvements of 1.06 in driving score and 4.7% in success rate over imitation learning, indicating that our reinforcement-based approach possesses strong generalization capabilities beyond the training distribution.

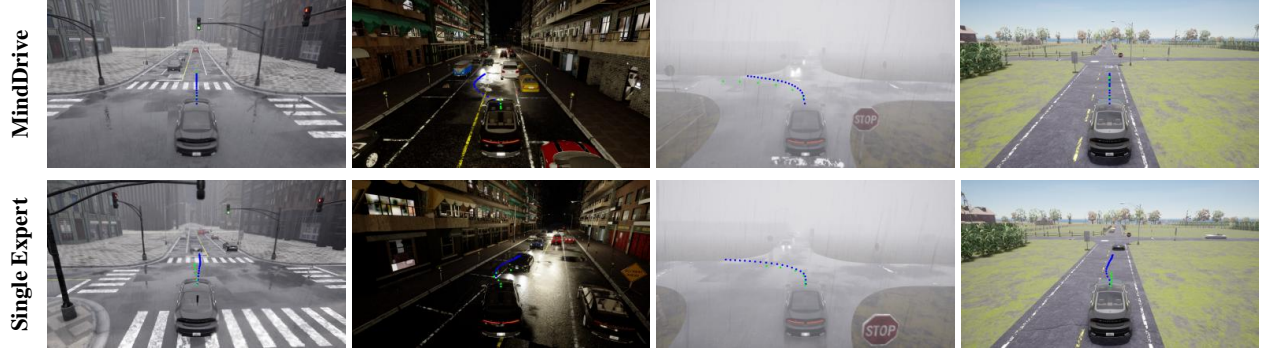


Figure A5. Comparison of our method with the single expert approach. Using a single expert results in poor trajectory quality and degraded control.

D.3. More Qualitative Results

We conduct a more comprehensive comparison between our method and imitation learning. As shown in Fig. A6, the integration of reinforcement learning (RL) leads to a noticeable improvement in task success rate, demonstrating the effectiveness of RL-based optimization in enhancing decision-making capabilities within interactive scenarios.

We also visualize the model’s output during the reasoning phase, as shown in Fig. A7. Our model maintains the integrity of reasoning throughout the policy update process, demonstrating that our approach effectively performs reinforcement at the semantic level without compromising high-level cognitive functions.

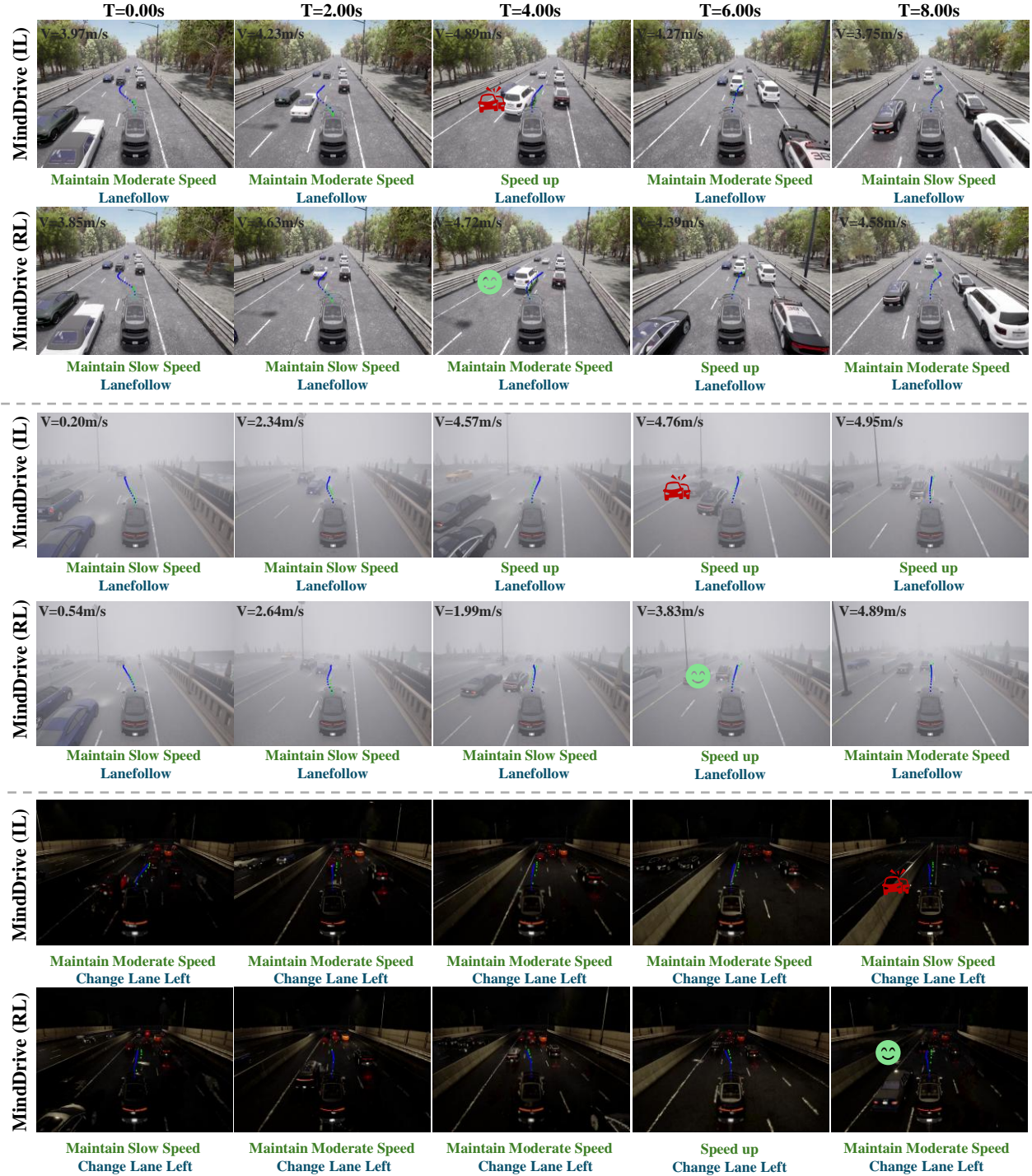
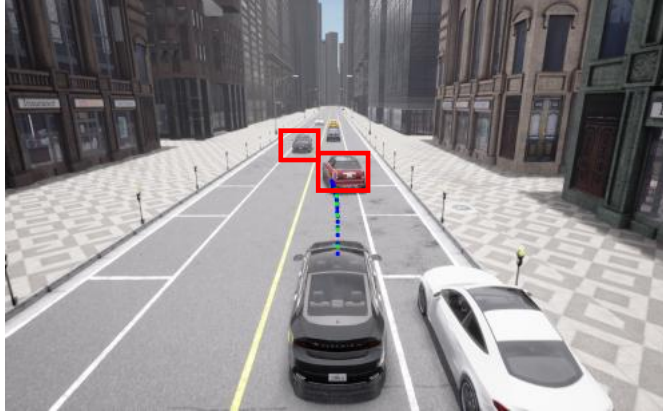


Figure A6. Comparison of our method with IL and RL.



Users: Can you describe the current weather conditions and the general environment depicted in the images?

MindDrive: The scene depicts an urban street flanked by tall buildings with a clear sky overhead. The road is dry and well-maintained, with multiple lanes separated by dashed lines. A red sedan is directly ahead in the same lane as the ego vehicle, maintaining a steady pace. The surrounding area appears calm with no immediate traffic congestion or pedestrians visible.

Users: Which objects in the scene are critical, and what effects do they have on the ego vehicle's movement?

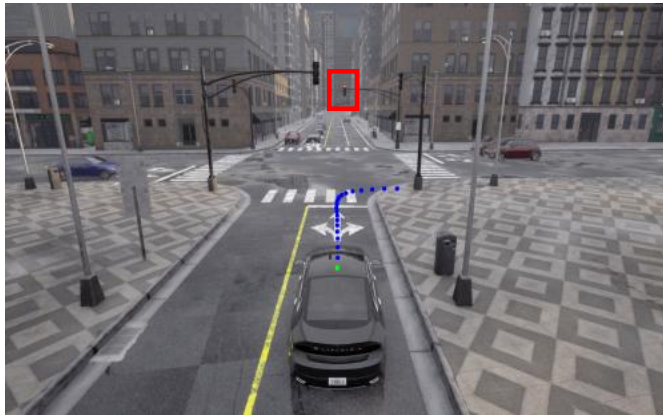
MindDrive : Car at $\langle -0.30, 12.56 \rangle$ is 12.56 meters ahead and slightly to the left, moving at a similar speed, may influence following distance. Car at $\langle -3.11, 25.11 \rangle$ is 25.11 meters ahead and slightly to the left, moving in the opposite direction, may influence lane changing.

Users: Please describe your driving behavior and explain the reasons.

MindDrive : You should maintain slow speed and follow the lane. The decision to maintain slow speed is influenced by the presence of the car directly in front of the ego vehicle, which is moving at a similar speed. The car in the opposite lane is moving faster, so changing lanes would not be advisable at this moment.

Users: What actions should the car be taking?

MindDrive : $\langle \text{maintain_slow_speed}, \text{lane_follow} \rangle$



Users: Can you provide a summary of the current driving scenario based on the input images?

MindDrive: The scene depicts an urban street intersection during daytime with clear weather. The traffic light ahead is red, indicating that vehicles must stop. There are no pedestrians visible in the crosswalks. The road surface appears smooth and well-maintained. A few vehicles are present in the distance, but none are immediately adjacent to the ego vehicle.

Users: Can you pinpoint the critical objects in the scene and describe their relation to the ego vehicle?

MindDrive : Traffic light at $\langle -1.72, 28.09 \rangle$ showing red, requiring the ego vehicle to stop.

Users: Please describe your driving behavior and explain the reasons.

MindDrive : You should stop and follow the lane. The red traffic light requires the ego vehicle to come to a complete stop before the crosswalk.

Users: What actions should the car be taking?

MindDrive : $\langle \text{stop}, \text{lane_follow} \rangle$

Figure A7. Qualitative results for scene understanding and action reasoning on Bench2Drive close-loop validation. The red indicates the critical objects influencing the action of the ego vehicle.